

European Satellite Benchmark for Control Education and Industrial Training

Francesco Sanfedino* Paolo Iannelli* Daniel Alazard*
Émilie Pelletier** Samir Bennani*** Bénédicte Girouart**

* *Fédération ENAC ISAE-SUPAERO ONERA, Université de
Toulouse, 10 Avenue Edouard Belin, BP-54032, 31055, France
(e-mail: francesco.sanfedino@isae.fr).*

** *European Space Agency ESA/ESTEC, Keplerlaan 1, 2201 AZ,
Noordwijk, The Netherlands*

*** *[Retired] European Space Agency ESA/ESTEC*

Abstract: To overcome the innovation gap of the Guidance, Navigation and Control (GNC) design process between research and industrial practice a benchmark of industrial relevance has been developed and is presented. This initiative is driven as well by the necessity to train future GNC engineers and the GNC space community on a set of identified complex problems. It allows to demonstrate the relevance of state-of-the-art modeling, control and analysis algorithms for future industrial adoption. The modeling philosophy for robust control synthesis, analysis including the control architecture that enables the simulation of the mission, i.e. the acquisition of a high pointing space mission, are provided.

Keywords: Dynamic Modeling, Uncertainty Modeling, Robust Control, Non-linear Simulation, Controls benchmark, Multi-Physics Modeling, Worst Case Analysis

1. INTRODUCTION

As reported by Dennehy et al. (2022), guidance, navigation, and control of aerospace systems is growing more complex together with a need of increased system performance. Over the last decades, academic research developed several solutions to address this need in modeling, control and validation and verification (V&V) areas. What is lacking nowadays is: a systematic transfer of these technologies to the industrial world, the scaling up of these advanced analysis and control algorithms to complex industrial benchmarks and the training of the future control engineers to deal with control problems of industrial complexity. High pointing space missions (Dennehy and Alvarez-Salazar (2018)) represent the perfect scenario in which GNC design encounters the hard task of coping with challenging high-level specifications and limitations imposed by the other spacecraft sub-systems (structure, thermal, optics, propulsion, etc.). In order to push the overall system to the limits of achievable performance, it is in fact necessary to predict in a preliminary design phase the worst-case configurations, due both to uncertainty in the system knowledge and mission operation conditions. NASA was a pioneer in the field of the integrated modeling philosophy. Young et al. (1979) were one of the first to investigate the fully coupled thermal/structure/control analysis problem. This philosophy was then employed in several NASA projects, from the Space Interferome-

try Mission (Grogan and Laskin (1998)), to the James Webb Space Telescope (Levine et al. (2023)). European Space Agency and industry investigated as well multi-disciplinary model-based system representation for end-to-end pointing performance characterization and optimization. Several missions, from the SILEX experience (Perez et al. (1989)) to the recent Euclid Mission (Racca et al. (2016)), benefited of this approach. The difficulty in practice of correctly conducting worst-case analysis for multi-disciplinary projects lies in their sequential approach, which is commonly followed in industry. Different tools are in fact employed for each area of expertise (GNC, structures, optics, etc.) and worst-case analyses are done in parallel in each field before reaching the final design. This results in many sub-iterations for the exchange of evolving inputs/outputs and trade-offs among different departments and consequent re-validation (Sanfedino et al. (2023a)). A unique user-friendly tool able to incorporate all possible plant configurations (dictated by the particular mission) is then needed to control engineers in order to shortcut this process, synthesize robust control strategies and fast validate system stability and performance. With this philosophy in mind, the Satellite Dynamics Toolbox library (SDTlib) (Alazard and Sanfedino (2020); Sanfedino et al. (2023b)) was conceived in order to build a complex multi-body spacecraft in the Two-Input Two-Output Port (TITOP) formalism (Alazard et al. (2015)) as a Linear Fractional Transformation (LFT) (Zhou et al. (1995)) model by analytically including any uncertain and variable physical parameter. By having a look to Fig. 1, structural components coming from analytical models or numerical Finite Element Model (FEM) analysis (imported from NASTRAN) can be directly connected together with

* This research was funded by the European Space Agency in the frame of the project "Generic Satellite Simulation & Analysis Tool: Dynamics Modelling, Controls and Validation of Complex Satellite Systems with Guaranteed Robust Pointing Performances": ESA Contract No. 4000141060/23/NL/MGu

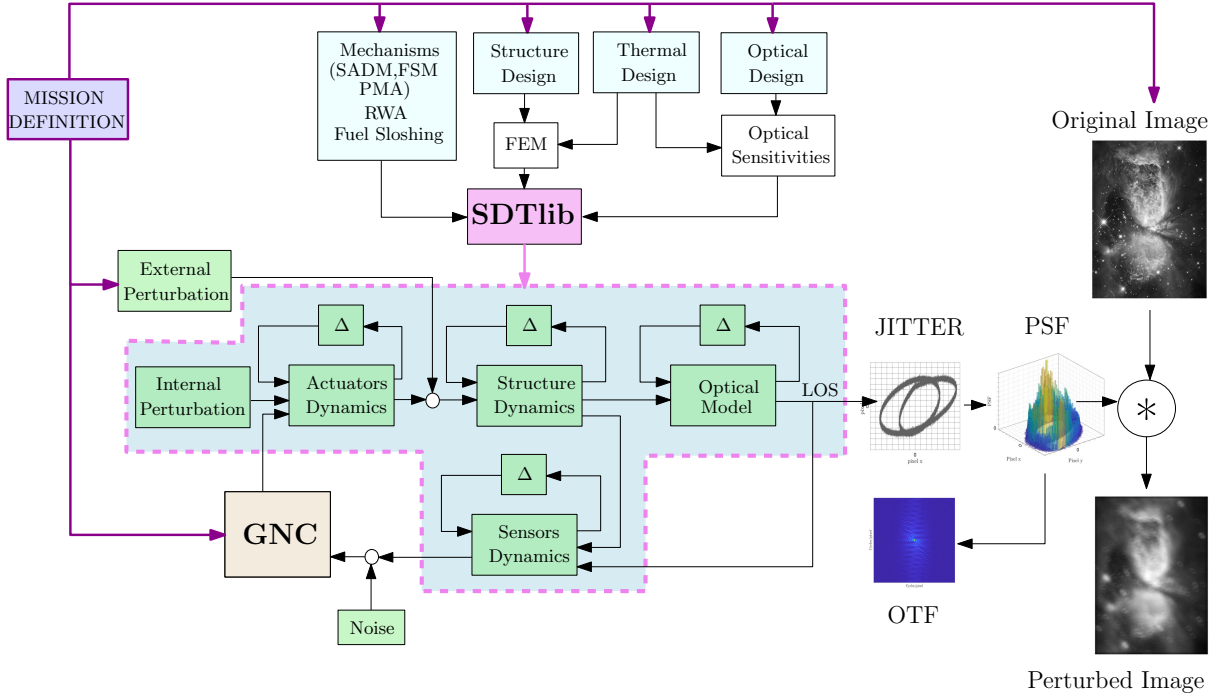


Fig. 1. Integrated Design Logic. Hubble Image: ©ESA/NASA.

mechanism models (like Solar Array Drive Mechanism (SADM), Reaction Wheel Assembly (RWA), Fast Steering Mirror (FSM), etc.), sloshing phenomena, chemical propulsion and analytical optical models. Variation and uncertainties of the overall system can be easily taken into account to model:

- uncertainties coming from preliminary hypotheses on mission design parameters,
- uncertainties coming from not guaranteed FEM validation on Earth in non-operative conditions (no micro-gravity, simulation of space environment on Earth),
- uncertainties coming from misknowledge of sensors and actuators models
- varying parameters like orientation of flexible appendages or speed of rotating elements (to correctly take into account gyroscopic effects).

For the mechanisms, it is also possible to take into account internal disturbances like static and dynamic imbalances of reaction wheels and harmonic perturbations due to SADM stepper commands, which have to be taken into account for microvibration compensation. Another feature available in SDTlib is the possibility to build models with the minimum number of occurrences of uncertain and variable parameter by construction and to pre-process the final model (ready for control synthesis and analysis) in order to eliminate non-physical states and reduce the model complexity. This functionalities are particularly interesting when the model has to be used for robust control synthesis (H_2/H_∞ - synthesis) or formal robust stability/performance analysis (μ or IQC analysis).

The benchmark proposed in this paper is constituted of:

- A scalable analysis and synthesis model (an LFT model of a complex telescope Space mission generated by SDTlib) to enable to perform tasks at various levels of granularity

- An equivalent non-linear high-fidelity simulator developed in Simscape and validated with SDTlib for time domain V&V.

Note that the user is asked to set the granularity of the model to be considered. The corresponding SDTlib and Simscape models will be then automatically generated. For instance the user can choose to get a model for the synthesis of a coarse pointing performance and choose the sensors/actuators among the ones available and set the degree of fidelity for the non-linear simulator (i.e. for the reaction wheels, one can choose to include static and dynamic imbalances, saturation, friction and/or friction spikes). See Section 3 for more details.

The optical benchmark can be used for several research problems and applications as listed below (not exhaustive list):

- End-to-end control synthesis and analysis process for stringent pointing requirements as proposed in Dennehy et al. (2022)
- Parametric sensitivity analysis as proposed in Kassarian et al. (2024) in order to reduce the number of most impacting uncertainties on closed-loop stability and performance analysis and better understand the physical meaning of possible worst-case configurations
- Deterministic or probabilistic μ -analysis as proposed respectively by Roos (2013) and Roos et al. (2024); and with application to flight data in Simplício et al. (2016)
- Integral Quadratic Constraints (IQC) analysis as in Veenman et al. (2021) and Pfifer and Seiler (2015)
- Non-linear validation algorithms based on global optimization techniques as proposed by Marcos et al. (2013)
- Classical fully non-linear Monte-Carlo V&V campaigns
- Multi-disciplinary optimization as proposed by Sanfedino et al. (2023c)
- Line-of-sight estimation with different combinations of sensors/actuators as in Sanfedino et al. (2022b)

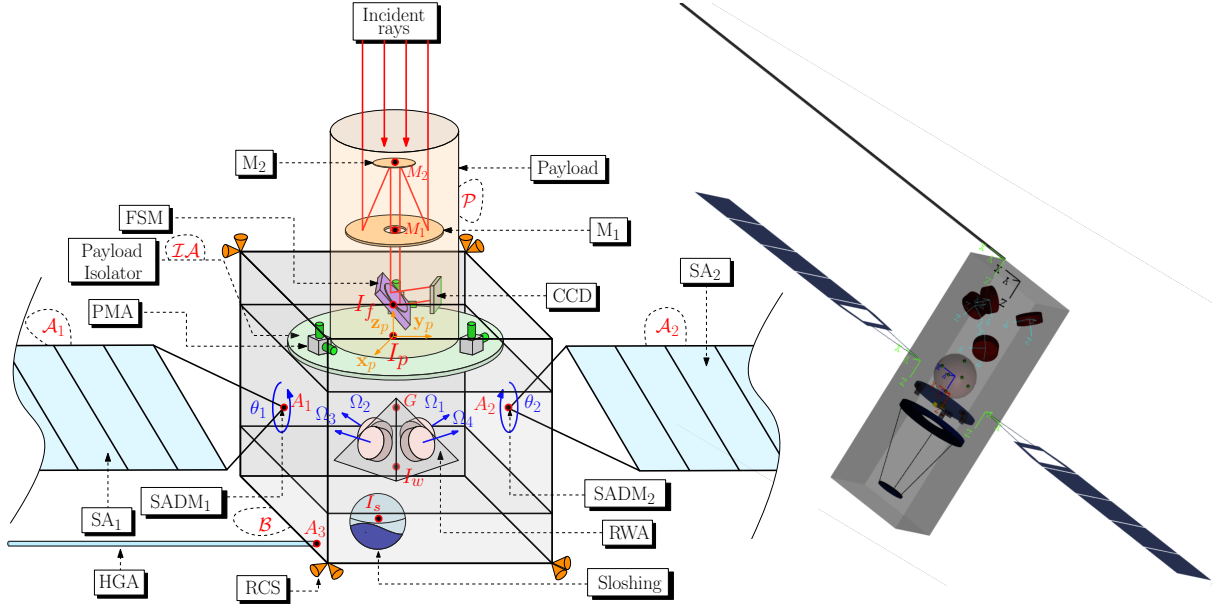


Fig. 2. Schematics of the benchmark SPCM (left) and equivalent view in Simscape Mechanical Explorer (right).

- Rigorous analysis (Biannic et al. (2010)) of transition between two different control modes (switching)
- Exploration of new architectures for actively controlling the spacecraft during Science phase without stopping disturbance sources (like reaction wheels) in order to optimize the science time window as shown in Sanfedino et al. (2022b)
- Generation of time domain data for any other applications (i.e. data driven control, system identification).

2. BENCHMARK ARCHITECTURE

A schematic of the proposed spacecraft model, the Satellite Pointing & Control Model (SPCM), is shown in Fig. 2. It includes a central bus \mathcal{B} connected to two rotating flexible solar arrays $\{\mathcal{A}_1 \mathcal{A}_2\}$, driven both by a SADM, a High-Gain Antenna (HGA) boom respectively at the interface point A_1 , A_2 and A_3 and an optical payload system \mathcal{P} . The optical payload is composed of a structure connecting the optical elements: the two mirrors M_1 and M_2 , the Charge-Coupled Device (CCD) and a an FSM. This payload is linked to the main body through a passive/active isolator. The isolation assembly ($\mathcal{I}\mathcal{A}$) interfaces the payload with the spacecraft bus with the objective of reducing the microvibration transmission from internal disturbance sources, reaction wheels (RWs) and SADMs, to the instruments. The passive damping typically makes use of visco-elastic materials, springs or hydraulic dampers isolator and it is modelled, in the context of the benchmark, with a 6-DoFs spring-damper system placed at the interface node I_p . On the other hand, the payload active isolation can be implemented by relying on a set of inertial proof-mass actuators (PMAs) that directly provide the action to actively counteract microvibrations in the middle-range frequency band as proposed in Sanfedino et al. (2022b). Each reaction wheel is connected to the main bus through a dedicated passive isolator, not shown in the figure for better clarity. Finally, a tank is connected to the spacecraft hub at the interface node I_s to account for the effect

of sloshing on the system's dynamics via an equivalent mechanical model (see Rodrigues et al. (2023)).

2.1 AOCS

The Attitude and Orbit Control System is equipped with:

- A set of 4 RWs wheel in pyramidal configuration
- A Reaction Control System (RCS). The RCS is a cluster of thrusters that typically provide higher control authority over the spacecraft attitude with respect to RWs. The use of a Micro-Propulsion System (MPS) can prevent/reduce the impact of microvibrations produced by RWs. The pointing performance that can be achieved depend on the thruster control authority and accuracy which is driven by the minimum impulse bit level; furthermore, these are often operated using Pulse-Width Modulation (PWM) strategies thus introducing non-linearities and limit cycle oscillations.

The AOCS sensors suite comprises:

- A *star tracker* (*STR*) system for attitude measurements.
- A *gyro* (*GYR*) system for angular velocity measurements. Two gyro assemblies are made available in the benchmark: a coarse pointing gyro (denominated as GYR-c) and an high performance one (GYR-f) that could be used during fine pointing operations.
- A *Fine Guidance Sensor* (*FGS*) which provides very precise attitude measurements necessary to cope with the tight pointing requirements needed during observations. The FGS is generally positioned near the main instrument and shares its Line-Of-Sight (LOS) in order to limit as much as possible thermo-elastic deformations that can worsen the LOS alignment between the instrument and FGS. The FGS is characterized by a reduced field of view and long image exposure time to provide a sufficient Signal-to-Noise Ratio for star detection.

2.2 Structure Dynamics

Finite element models of complex structural elements, like the HGA, the solar arrays and the optical payload are

analyzed in MSC NASTRAN (see Fig. 4) and directly included in the multi-body SDTlib environment. SDTlib allows also to retrieve the data needed for the Simscape Reduced Order Flexible Solid (ROFS) as shown in Sanfedino et al. (2023a). All mechanisms are modeled as well in SDTlib and in Simscape environment. Figure 3 shows for example a comparison of the singular values of the transfer function from the wheel harmonic disturbance to the main hub angular accelerations, where the difference between the two models, depicted by the green lines, is obtained by sampling several configurations of the reaction wheels' speeds.

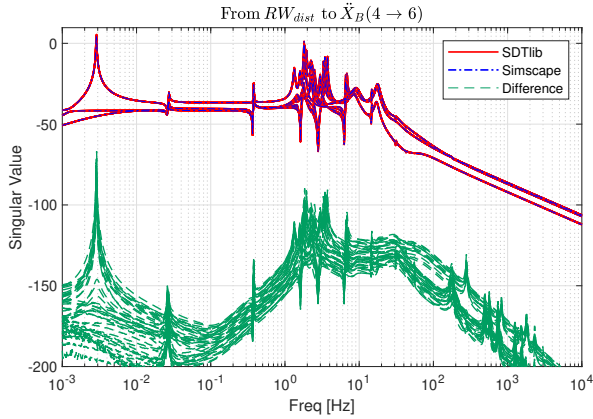


Fig. 3. Singular Values of the transfer function from the wheels' harmonic disturbances to the main hub angular accelerations.

2.3 Optical Design

The optical payload chosen for the benchmark is a Ritchey-Chrétien two-mirror telescope system as shown in Fig. 4, where both the primary and secondary mirrors are hyperboloids. The FSM is then placed at half the back focal distance to rotate the beam towards the detector located on the focal plane. The ray-tracing algorithm in Redding and Breckenridge (1991) is used to derive the analytical linear optical sensitivities under the paraxial approximation (or small angle approximation). The LOS is then computed by considering an incident ray entering the system along the LOS direction and incident in the centroid of the primary mirror. Since computing the contribution of the optical surfaces' deformation to the Wave Front Error (WFE) is outside the scope of the benchmark and would require the use of numerical solutions provided by dedicated software, an averaged motion of the primary mirror with a *virtual* point positioned at the vertex of the primary mirror is used to address LOS errors.

2.4 External and internal Disturbances

The telescope is supposed to be rotating on a circular orbit, where gravity gradient and solar pressure torques acts on the spacecraft by perturbing its attitude at very low frequency in the AOCS bandwidth. Internal disturbances coming from the use of SADM and reaction wheels and are taken into account. In particular as multiple harmonic perturbation due to its microstepping driver is considered at the input of the output shaft holding the solar array as in Sanfedino et al. (2022a). For the reaction wheels,

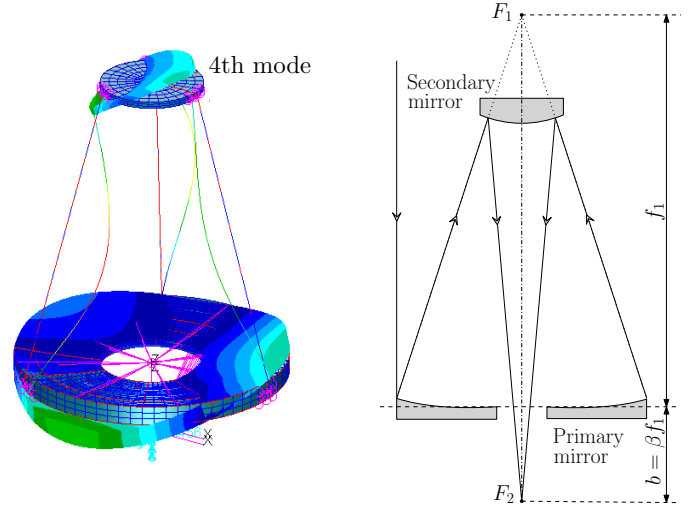


Fig. 4. Ritchey-Chrétien two-mirror telescope system: finite element analysis in Nastran (left) and schematics (right)

static and dynamic imbalances together with a broadband noise are modeled. In particular the benchmark can be used in order to characterize the influence of each wheel acceleration to the input disturbance in microgravity conditions and taking into account coupling with the rest of the spacecraft structure as shown in Fig. 5. In the non-linear simulator Stribek-like friction Olsson et al. (1998) and friction spikes Ehinger et al. (2015) of the wheels can be also taken into account.

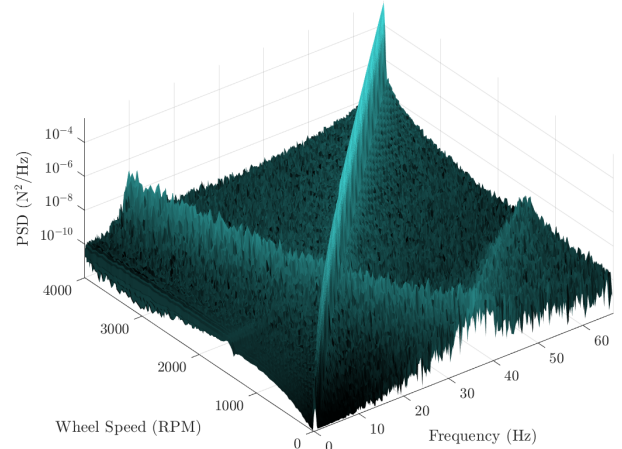


Fig. 5. Reaction wheel waterfall plot of the disturbance torque measured in the wheel reference frame. Note the nutation modes of the wheel isolator varying with the wheel speed.

2.5 Propulsion

The propulsion system is constituted by 12 thrusters in parallelepiped configuration. The PWM function is build taking into the Minimum Impulse Bit (MIB) and following model presented in Ieko et al. (1999).

2.6 Stability and Performance metrics

System stability has to be guaranteed in all phases of the mission. Classical criteria (i.e. SISO gain, phase, delay margins) and more advanced ones (i.e. robust MIMO

modulus and disk margins) can be easily imposed. Pointing performance are imposed on the different phases of the mission (as detailed in Section 3) by following ESA standards (ESA (2015)) based on Pittelkau and McKinley (2012). Metrics as the Absolute Performance Error (APE), the Relative Performance Error (RPE) and the Performance Drift Error (PDE) are used to define the expected performance on the image quality, dependent on the camera integration time. This pointing performance has to cope as well with stability requirements and performance limitation imposed by sensor/actuator noise and actuation authority. Other criteria can be easily added by the user: control bandwidth, rise time, overshoot, settling time, roll-off, peak gain, discretization, quantization and advanced criteria expressed in various other metrics for MIMO, time varying and nonlinear uncertain systems.

3. MISSION DEFINITION AND USER SETTINGS

Within the various operational modes of the spacecraft, a particular problem is specifically designed as a use case to challenge the future users on the same scenario. This does not limit the use of the present benchmark to other possible investigations as described in Section 1. Figure 6 depicts the timeline for the proposed use case, outlining a sequence of mission phases designed to reach the final science phase which requires precise pointing accuracy and stability to enable observations of a specific target (note that the user is free to select the most suited combination of sensors/actuators proposed in the figure):

Window 1 - slew transient: The timeline of the proposed benchmark starts at time t_0 and it is initially assumed that the spacecraft performs a slew maneuver to point the payload LOS to the target. Such transient shall be optimized in terms of agility, reduction of the tranquilization time and final attitude error (APE₁).

Window 1 - slew steady state: A first APE requirement (APE₁) has to be met during this phase in order to provide the conditions for the mode switching and the transition to the coarse pointing phase. The duration of the slew steady state is considered fixed and equal to \tilde{t}_1 .

Window 2 - Coarse pointing transient: After the specification APE₁ is verified at the end of the slew, the mode switching to the control architecture for coarse pointing control is initiated. This switching involves both the transition from the slew controller to the coarse pointing control scheme and potentially also an AOCS architectural transition (i.e. RCS → RWs). This transient ends when the spacecraft fulfill the requirements for coarse pointing steady state operations.

Window 2 - Coarse pointing steady state: The coarse pointing phase is envisioned as an intermediate phase in order to provide the sufficient pointing conditions for the initial hand over from star trackers to the FGS and subsequent transition from coarse to fine pointing control architecture. In this phase requirements are provided both in terms of instantaneous and window error indexes (APE₂ and RPE₂). The duration of the coarse pointing steady state is considered fixed and equal to \tilde{t}_2 .

Window 3 - Fine pointing transient: In this phase the hand over to the fine guidance control architecture is initiated. An FGS and high-performance gyro can be activated to provide precise attitude determination, while

a second actuator switch at hub level can be envisioned (i.e. from RWs to a MPS). Furthermore, a combination of actuators and sensors at payload level can be incorporated in the control architecture to guarantee the required pointing performance for the optimal execution of the science observation.

Window 3 - Fine pointing steady state: The fine pointing phase (science observation phase) presents the most challenging aspects for the AOCS and LOS stabilization system in terms of pointing requirements and complexity of the overall control architecture. Indeed, besides more stringent instantaneous and windowed requirements (APE₃ and RPE₃) with respect to the previous phase, a windowed-stability requirements in the form of Performance Drift Error (PDE) is imposed during science observation (PDE₃). The duration of the fine pointing steady state is considered equal to \tilde{t}_3 . The total time for

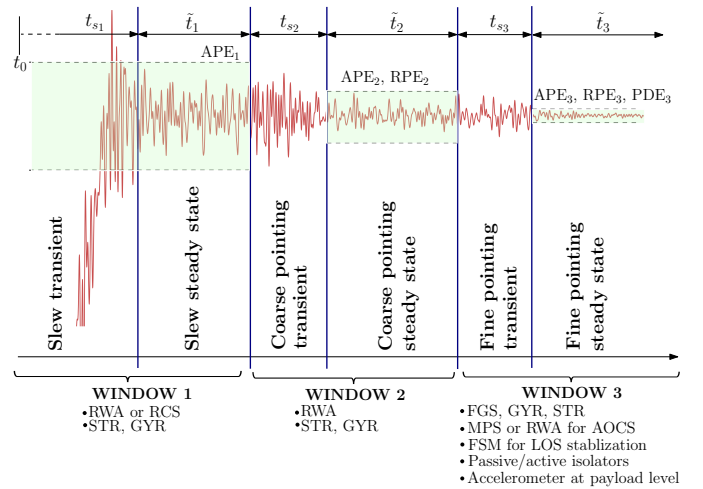


Fig. 6. Timeline sequence for the benchmark problem

the previous sequence is fixed and a baseline controller is provided to the user, who can directly plug his solution into the simulator. The challenge will be to maximize the science phase, meaning the fine pointing steady state duration \tilde{t}_3 . This means that the user has to propose a solution that optimizes the slew maneuver and the transitions between modes by coping with all uncertainties of the system and by facing non-linearities like saturations, reaction wheels imbalances, Stribek and spike frictions, SADM microstepping signals, PWM signals for thrusters and all measurement noises. Iannelli et al. (2024) extensively outlines all available settings to input data, how to retrieve SDTlib and Simscape models for different control modes, how to set actuators/sensors and how to run a simulation and obtain the automated reporting file.

4. CONCLUSION

A benchmark problem was presented with a threefold goal:

- training future GNC engineers with problems of industrial complexity;
- trading-off advanced control, analysis and validation tools applied to a realistic satellite control problem by stretching academic tools that often use to collapse on complex large scale problems or do become unduly hard to execute when applied in an industrial context;

- transferring to industry the state-of-the-art GNC tools to dramatically reduce the design iterations.

REFERENCES

- Alazard, D., Perez, J.A., Cumer, C., and Loquen, T. (2015). Two-input two-output port model for mechanical systems. In *AIAA GNC Conf.*, 1778.
- Alazard, D. and Sanfedino, F. (2020). Satellite dynamics toolbox for preliminary design phase. In *43rd Annual AAS GNC Conf.*, volume 30, 1461–1472.
- Biannic, J.M., Pittet, C., Lafourcade, L., and Roos, C. (2010). Lpv analysis of switched controllers in satellite attitude control systems. In *AIAA GNC Conf.*
- Dennehy, C. and Alvarez-Salazar, O.S. (2018). Spacecraft micro-vibration: a survey of problems, experiences, potential solutions, and some lessons learned. Technical report, Tech. Report NASA/TM-2018-220075.
- Dennehy, C., Bennani, S., Shankar, U., Vandersteen, J., VanZwieten, T., Von der Porten, P., Wolf, A., Girouart, B., and Casasco, M. (2022). Verification and validation (v&v) of guidance & control systems: Results from the first inter-agency workshop on gnc v&v. In *Proceedings of the 44th Annual AAS GNC Conf.*
- Ehinger, M., Meyer, P., Quintel, H., and Kupferschmitt, S. (2015). Mitigation of wheel friction torque instabilities - final report. Technical report, Rockwell Collins - ESA TRP Program.
- ESA (2015). Esa pointing error engineering handbook, handbook essb-hb-e-003.
- Grogan, R. and Laskin, R. (1998). On multidisciplinary modeling of the space interferometry mission. In *Proceedings of the 1998 ACC (IEEE Cat. No.98CH36207)*, volume 3, 1558–1562 vol.3.
- Iannelli, P., Sanfedino, F., and Alazard, D. (2024). Esa pointing benchmark, user-guide. Technical report, European Space Agency.
- Ieko, T., Ochi, Y., and Kanai, K. (1999). New design method for pulse-width modulation control systems via digital redesign. *JGCD*, 22(1), 123–128.
- Kassarjian, E., Sanfedino, F., Alazard, D., and Evain, H. (2024). Parametric sensitivity analysis for the robust control of uncertain space systems. In *CEAS EuroGNC 2024, Bristol, UK*.
- Levine, M., Mosier, G., Walsh, G., Blaurock, C., and Hartig, G. (2023). Integrated modeling of the James Webb Space Telescope: pre-launch predictions, flight performance, and lessons learned. In M.A. Kahan (ed.), *Optical Modeling and Performance Predictions XIII*, volume 12664, 1266409. SPIE.
- Marcos, A., Garcia De Marina, H., Mantini, V., Roux, C., and Bennani, S. (2013). Optimization-based worst-case analysis of a launcher during the atmospheric ascent phase. In *AIAA GNC Conf.*, 4645.
- Olsson, H., Åström, K.J., De Wit, C.C., Gäfvert, M., and Lischinsky, P. (1998). Friction models and friction compensation. *Eur. J. Control*, 4(3), 176–195.
- Perez, E., Bailly, M., and Pairo, J.M. (1989). Pointing Acquisition And Tracking System For Silex Inter Satellite Optical Link. In S. Gowrinathan (ed.), *Acquisition, Tracking, and Pointing III*, volume 1111, 277 – 288. SPIE.
- Pfifer, H. and Seiler, P. (2015). Integral quadratic constraints for delayed nonlinear and parameter-varying systems. *Automatica*, 56, 36–43.
- Pittelkau, M. and McKinley, W. (2012). Pointing error metrics: Displacement, smear, jitter, and smitter with application to image motion mtf. In *AIAA/AAS Astr. Spec. Conf.*
- Racca, G.D., Laureijs, R., Stagnaro, L., Salvignol, J.C., Alvarez, J.L., Criado, G.S., Venancio, L.G., Short, A., Strada, P., Bönke, T., Colombo, C., Calvi, A., and al. (2016). The Euclid mission design. In *Space Telescopes and Instrumentation 2016: Optical, Infrared, and Millimeter Wave*, volume 9904, 99040O. SPIE.
- Redding, D.C. and Breckenridge, W.G. (1991). Optical modeling for dynamics and control analysis. *JGCD*, 14(5), 1021–1032.
- Rodrigues, R., Sanfedino, F., Alazard, D., Preda, V., and Olucha, J. (2023). Linear parameter-varying gain-scheduled attitude controller for an on-orbit servicing mission involving flexible large spacecraft and fuel sloshing. In *12th ESA GNC Conference, Sopot, Poland*.
- Roos, C. (2013). Systems modeling, analysis and control (smac) toolbox: An insight into the robustness analysis library. In *2013 IEEE CACSD Conf.*, 176–181. IEEE.
- Roos, C., Biannic, J.M., and Evain, H. (2024). A new step towards the integration of probabilistic μ in the aerospace v&v process. *CEAS Space J.*, 16(1), 59–71.
- Sanfedino, F., Alazard, D., Kiley, A., Watt, M., Simplicio, P., and Ankersen, F. (2023a). Monolithic versus distributed structure/control optimization of large flexible spacecraft. In *12th ESA GNC Conf., Sopot, Poland*.
- Sanfedino, F., Alazard, D., Kassarjian, E., and Somers, F. (2023b). Satellite dynamics toolbox library: a tool to model multi-body space systems for robust control synthesis and analysis. *IFAC-PapersOnLine*, 56(2), 9153–9160. 22nd IFAC World Congress.
- Sanfedino, F., Alazard, D., Kiley, A., Watt, M., Simplicio, P., and Ankersen, F. (2023c). Robust monolithic versus distributed control/structure co-optimization of flexible space systems in presence of parametric uncertainties. *J. SMO*, 66(12), 247.
- Sanfedino, F., Alazard, D., Preda, V., and Oddenino, D. (2022a). Integrated modeling of microvibrations induced by solar array drive mechanism for worst-case end-to-end analysis and robust disturbance estimation. *J. MSSP*, 163, 108168.
- Sanfedino, F., Thiébaud, G., Alazard, D., Guercio, N., and Deslaef, N. (2022b). Advances in fine line-of-sight control for large space flexible structures. *J. AST*, 130, 107961.
- Simplicio, P., Bennani, S., Marcos, A., Roux, C., and Lefort, X. (2016). Structured singular-value analysis of the vega launcher in atmospheric flight. *JGCD*, 39(6), 1342–1355.
- Veenman, J., Scherer, C.W., Ardura, C., Bennani, S., Preda, V., and Girouart, B. (2021). Iqclab: A new iqclab based toolbox for robustness analysis and control design. *IFAC-PapersOnLine*, 54(8), 69–74.
- Young, J., Frisch, H., Jones, G., and Walker, W. (1979). Interactive analysis program activity. Large space systems technology 1st annual technical review, NASA, Scientific and Technical Information Office.
- Zhou, K., Doyle, J., and Glover, K. (1995). *Robust and optimal control*. Prentice hall Upper Saddle River, NJ.